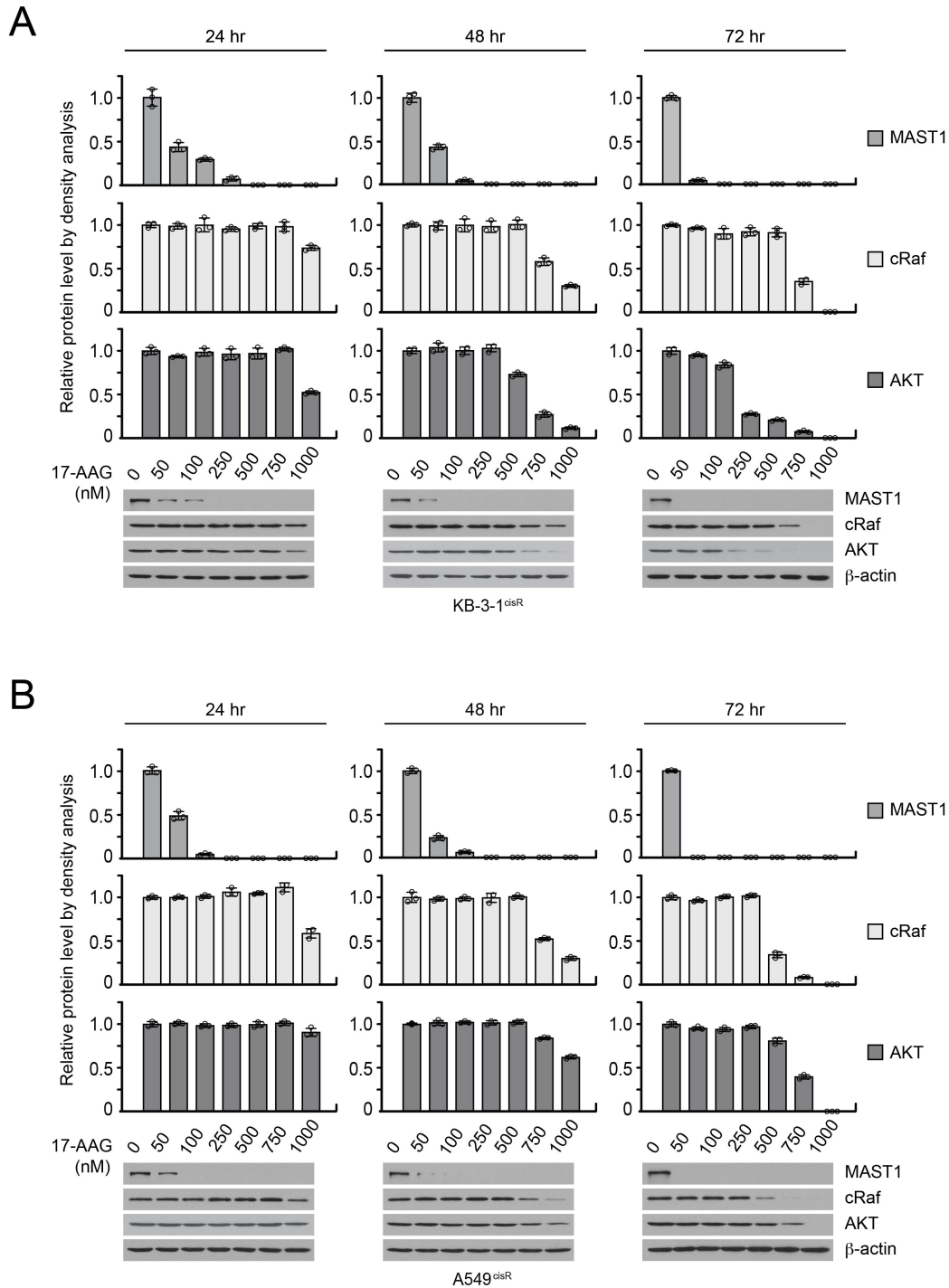
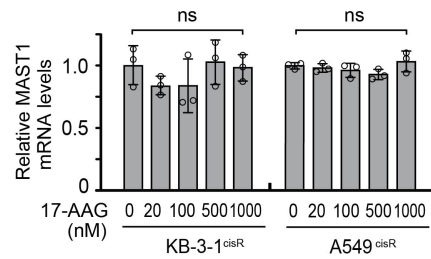


Hsp90B enhances MAST1-mediated cisplatin resistance by protecting MAST1 from proteosomal degradation

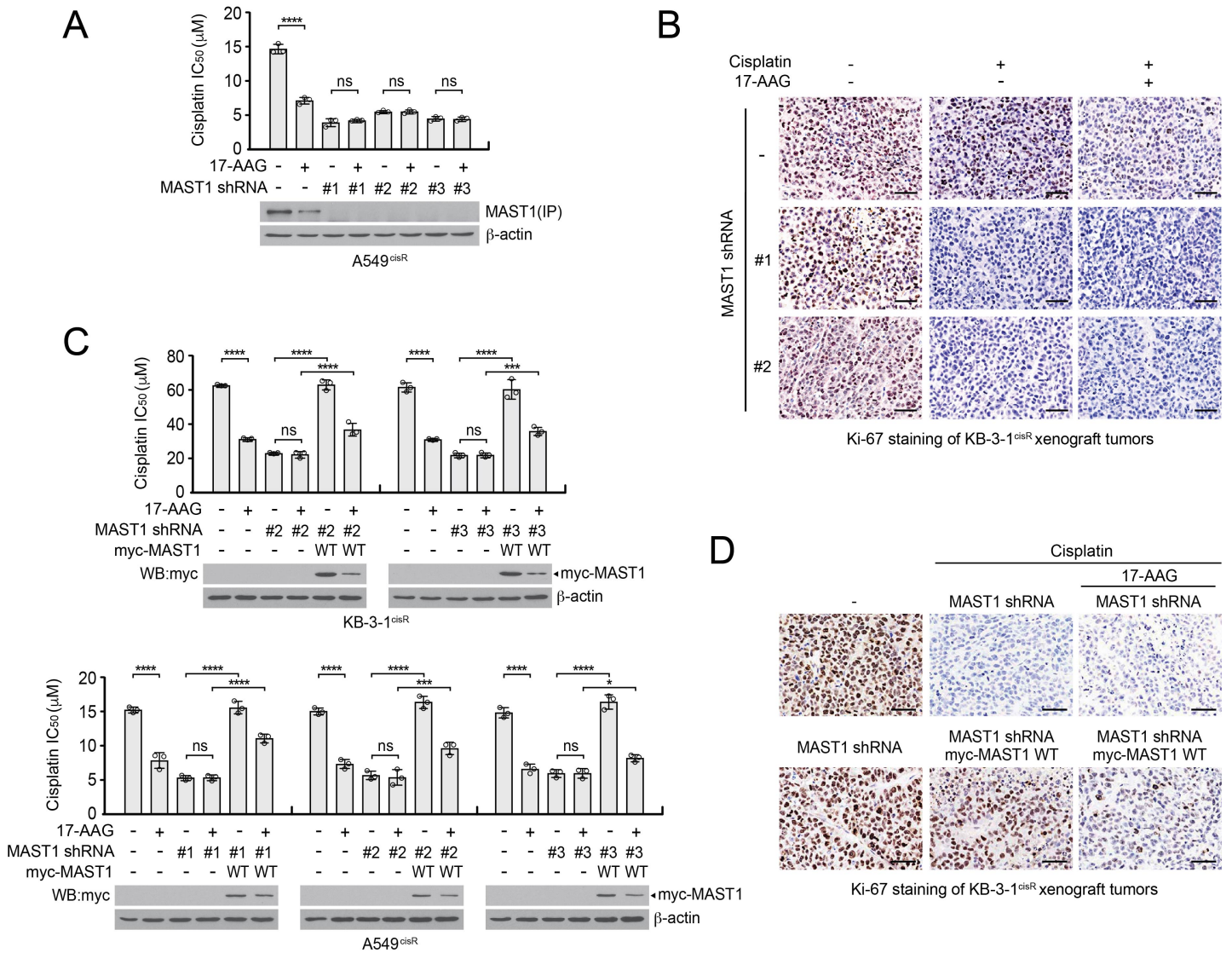
Pan et al.



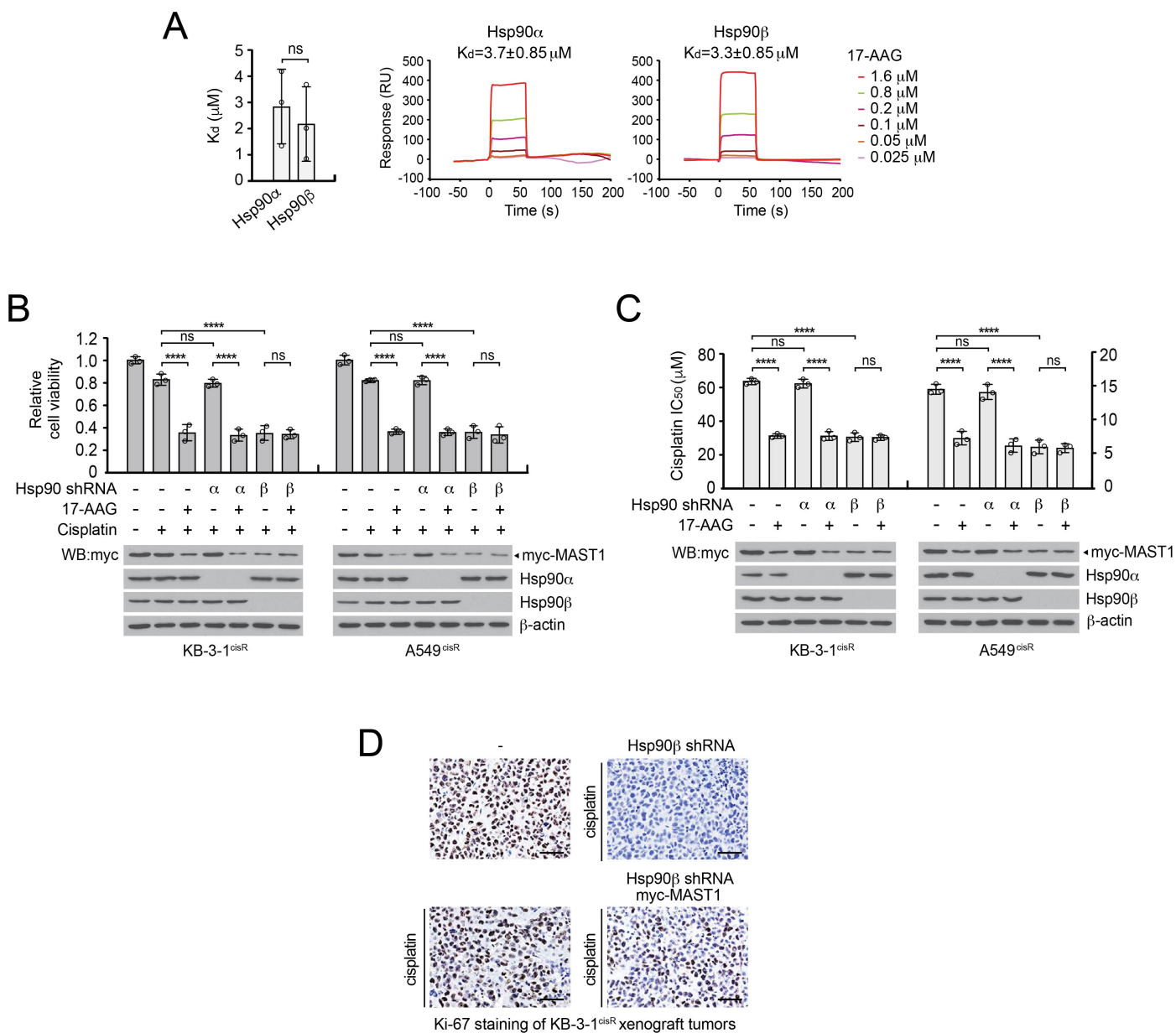
Supplemental Figure 1. MAST1 is more susceptible than cRaf or AKT to degradation by 17-AAG in cisplatin-resistant cancer cells. KB-3-1^{cisR} (A) and A549^{cisR} (B) cells were treated with 17-AAG at the indicated concentrations and time prior to immunoblotting. Protein levels were determined by densitometry analysis. Data are mean \pm SD from three technical replicates and representative of two independent biological experiments.



Supplemental Figure 2. Hsp90 inhibition does not alter MAST1 gene expression in cisplatin-resistant cancer cells. KB-3-1^{cisR} and A549^{cisR} cells were treated with increasing concentrations of 17-AAG for 24 h. MAST1 mRNA level was determined by quantitative RT-PCR. Data are mean \pm SD from three technical replicates and representative of three independent biological experiments. Statistical analysis was performed by 1-way ANOVA.

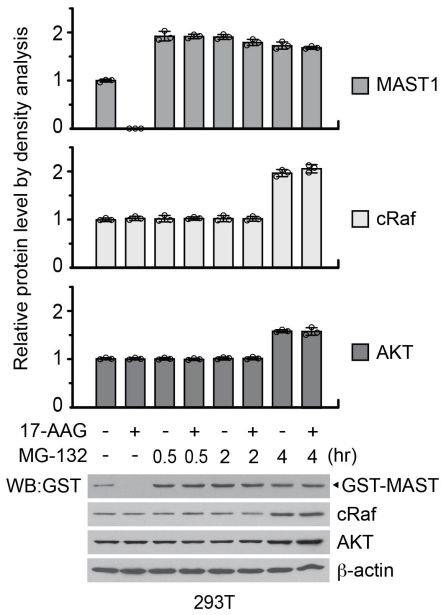


Supplemental Figure 3. 17-AAG treatment sensitizes cisplatin-resistant cancer cells to cisplatin through MAST1. (A) Cisplatin IC₅₀ upon 17-AAG treatment with or without MAST1 knockdown in A549^{cisR} cells. Cisplatin IC₅₀ values were determined by CellTiter-Glo assay. (C) Cisplatin IC₅₀ upon 17-AAG treatment, MAST1 knockdown, and rescue expression of MAST1 WT. Three different shRNA clones were used for MAST1 knockdown. (B and D) Effect of 17-AAG treatment and MAST1 knockdown (B), and knockdown and rescue expression of MAST1 WT (D) on tumor proliferation was assessed by Ki-67 immunohistochemistry (IHC) staining. Scale bars represent 50 µm. Data shown are representative of three (A and C) and two (B and D) independent biological experiments. Data are mean ± SD from three technical replicates. Statistical analysis was performed by 1-way ANOVA (**P*<0.05; ****P*<0.005; *****P*<0.0001).

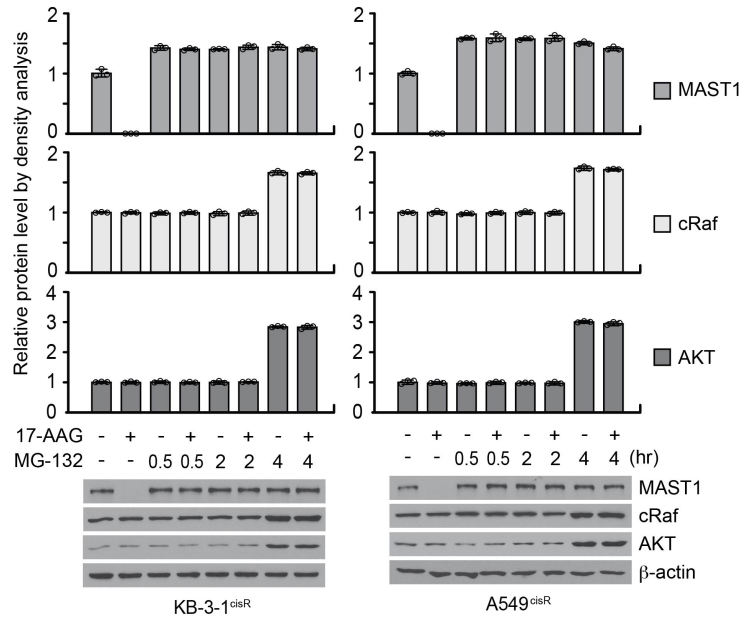


Supplemental Figure 4. Hsp90B stabilizes MAST1 and contributes to cisplatin resistance. (A) Interactions between hsp90 isoforms and 17-AAG were determined by Biacore SPR. **(B-C)** Effect of 17-AAG on MAST1 protein level, cell viability, and cisplatin response in cells with hsp90A or hsp90B knockdown. KB-3-1^{cisR} and A549^{cisR} cells with hsp90A or hsp90B knockdown were treated with 17-AAG (100 nM) in the presence of sublethal doses of cisplatin (KB-3-1^{cisR}: 5 μg/ml, A549^{cisR}: 2 μg/ml). **(D)** Effect of hsp90B knockdown and MAST1 overexpression on tumor proliferation. Scale bars represent 50 μm. Data shown are representative of three (A-C) and two (D) independent biological experiments. Data are mean ± SD from three technical replicates. Statistical analysis was performed by 1-way ANOVA (*****P*<0.0001).

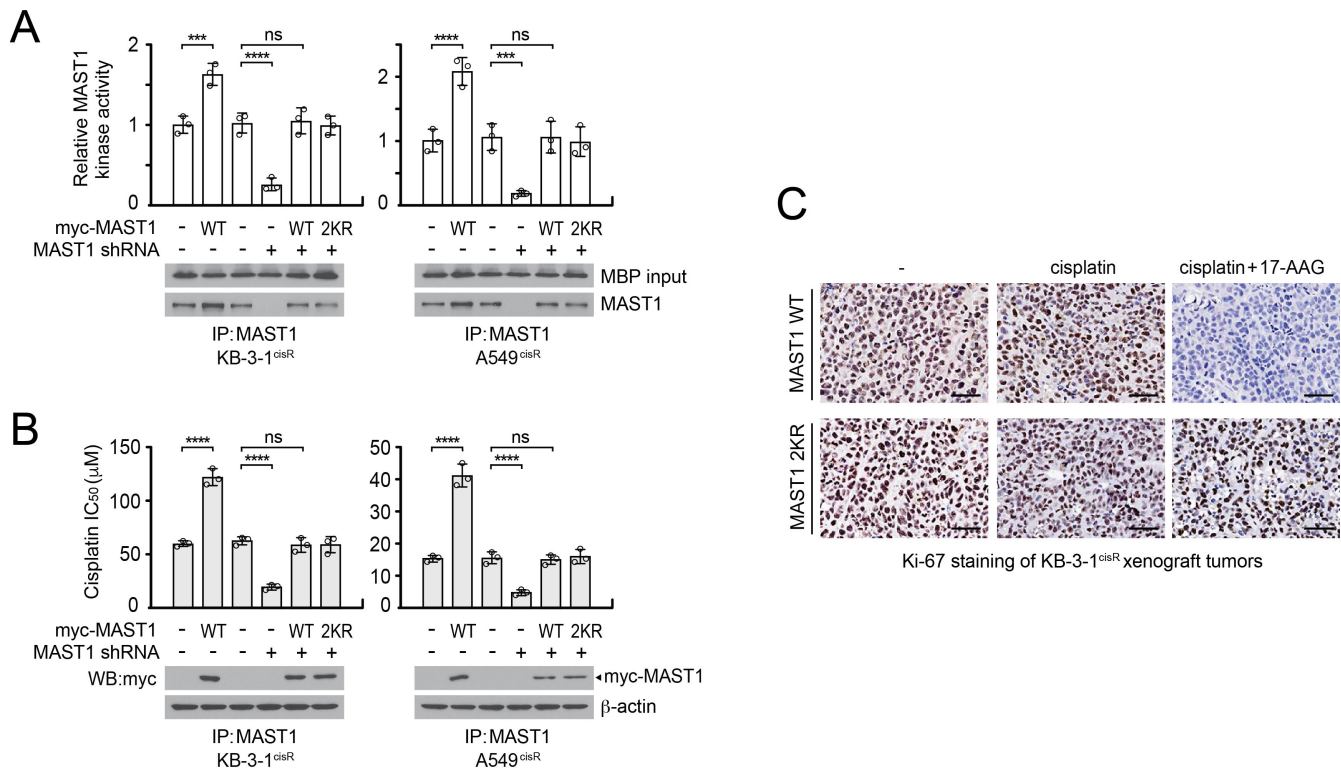
A



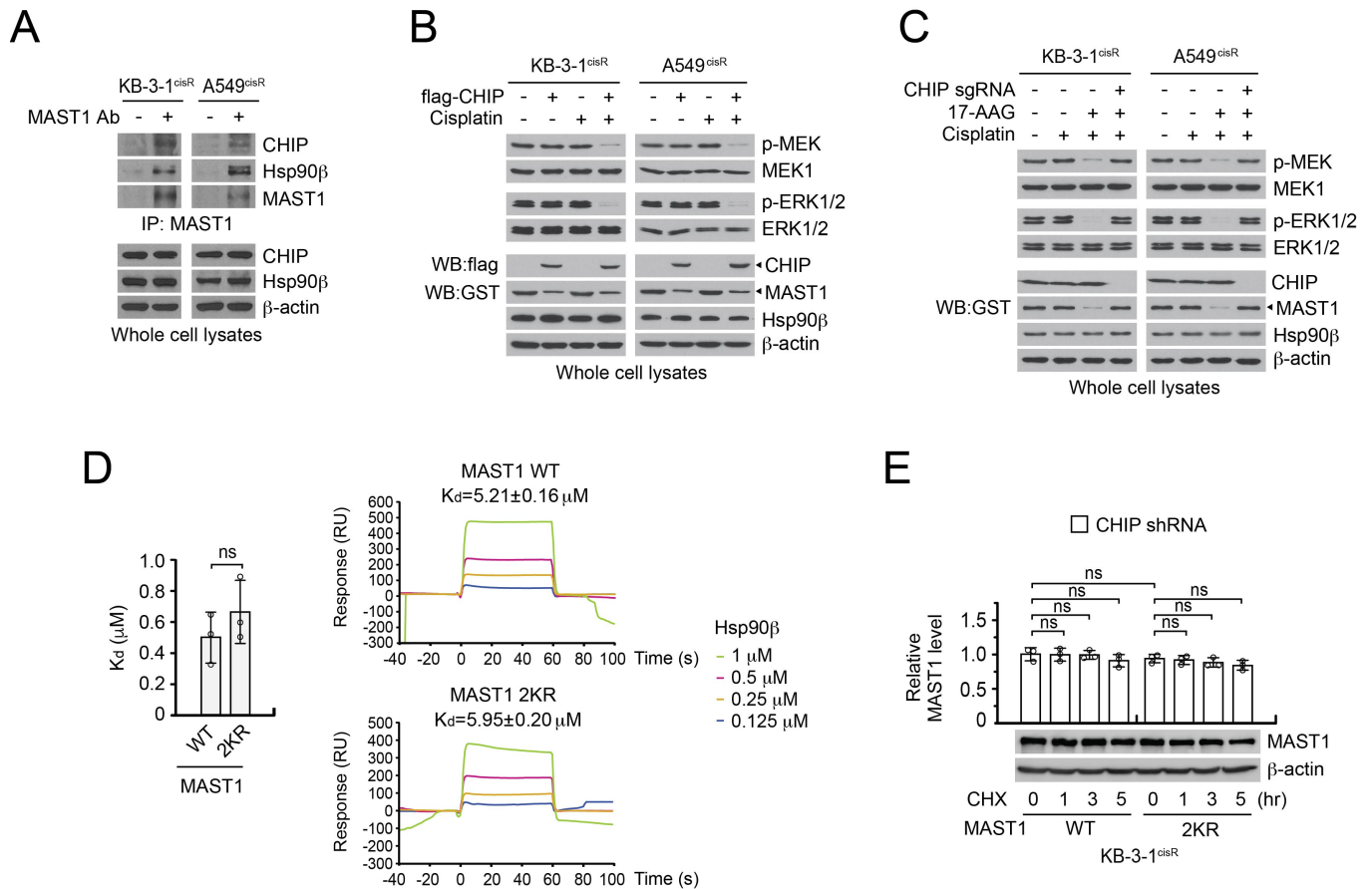
B



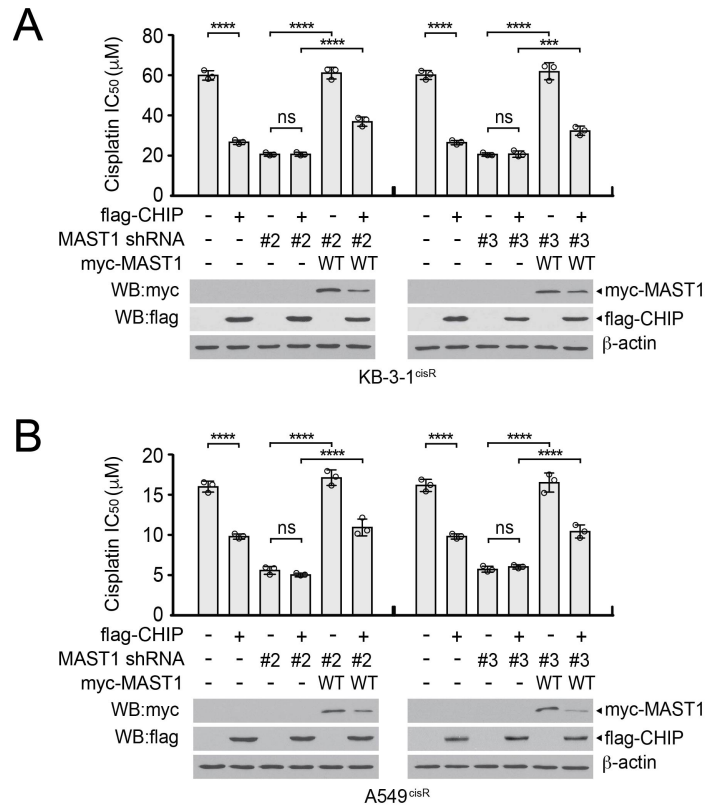
Supplemental Figure 5. Proteasome inhibitor MG-132 stabilizes hsp90 client proteins MAST1, cRaf, and AKT but with different sensitivities. 293T cells (A) or KB-3-1^{cisR} and A549^{cisR} cells (B) were treated with MG-132 (10 μM) for the indicated times before the addition of 17-AAG (1 μM) for 4 hours. Protein levels were determined by densitometry analysis. Data are mean ± SD from three technical replicates and representative of two independent biological experiments.



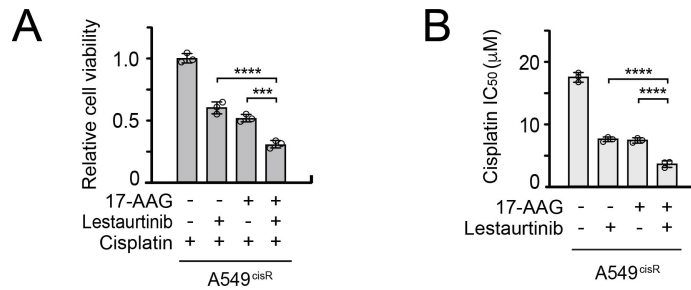
Supplemental Figure 6. MAST1 protein level contributes to MAST1 activity, cisplatin resistance, and tumor proliferation. (A-B) MAST1 kinase activity (A) and cisplatin IC₅₀ were determined in KB-3-1^{cisR} and A549^{cisR} cells with MAST1 modulation. MAST1 was enriched from cells by immunoprecipitation and MAST1 activity was assessed by ADP-Glo kinase assay using myelin basic protein (MBP) as a substrate. Cisplatin IC₅₀ was assessed by CellTiter Glo assay. **(C)** Effect of 17-AAG and MAST1 WT or 2KR expression on cisplatin-resistant tumor proliferation. Scale bars represent 50 μm. Data shown are representative of two independent biological experiments for (A)-(C) and are mean ± SD from three technical replicates for (A) and (B). Statistical analysis was performed by 1-way ANOVA (***)*P*<0.005; ****)*P*<0.0001).



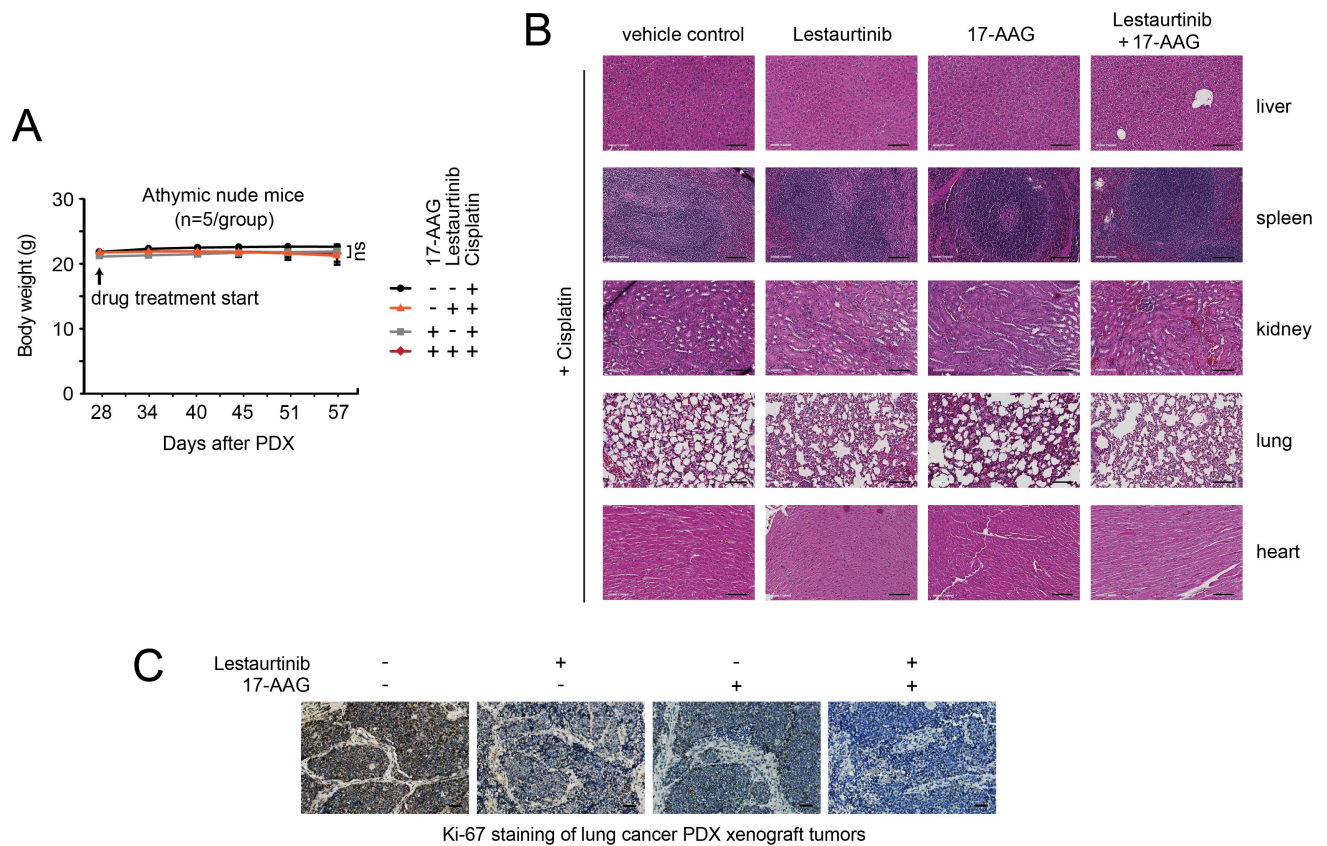
Supplemental Figure 7. MAST1 interacts with CHIP and hsp90B. (A) Endogenous interaction of CHIP, hsp90B, and MAST1 in cisplatin-resistant cancer cells. (B-C) Effect of CHIP overexpression (B) or knockout (C) on activation status of MAST1 downstream effectors, MEK1 and ERK1/2 in the presence or absence of cisplatin. Cells were treated with 5 mg/ml of cisplatin and 50 nM of 17-AAG for 48 hours. Activation of MEK1 and ERK1/2 was assessed by phosphorylation of MEK1 S217/S221 and ERK1/2 T202/Y204, respectively. (D) Interaction between MAST1 WT or 2KR and hsp90B was quantified by Biacore SPR analysis. Dissociation constants (K_d) values for MAST1 WT-hsp90B or MAST1 2KR-hsp90B interaction are compared. (E) Protein stability of MAST1 WT or 2KR in CHIP knockdown cells. Cells with CHIP knockdown were treated with 5 μ g/ml cycloheximide (CHX) for the indicated times. Data shown are representative of two (A-D) and one (E) independent biological experiments. Data are mean \pm SD from three technical replicates for (E). Statistical analysis was performed by two-tailed student *t* test for (D) and 1-way ANOVA for (E).



Supplemental Figure 8. CHIP-mediated degradation of MAST1 sensitizes cisplatin-resistant cells to cisplatin. Effect of MAST1 WT rescue expression on cisplatin sensitivity and MAST1 protein level in KB-3-1^{cisR} (A) and A549^{cisR} (B) cells with CHIP overexpression and MAST1 knockdown. Two distinct shRNA clones (#2 and #3) were used for MAST1 knockdown. Cells with flag-CHIP and MAST1 knockdown or WT overexpression were treated with increasing concentrations of cisplatin for 48 h. Cell viability was measured by CellTiter-Glo assay and cisplatin IC₅₀ was calculated using Graphpad Prism 8. Data are mean ± SD from three technical replicates and representative of three independent biological experiments for (A) and (B). Statistical analysis was performed by 1-way ANOVA (***P*<0.005; *****P*<0.0001).



Supplemental Figure 9. Cisplatin-resistant cell viability is further decreased by 17-AAG and lestaurtinib combination. Effect of combinatorial treatment with 17-AAG and lestaurtinib on cell viability (A) and cisplatin sensitivity (B). A549^{cisR} cells were treated with 17-AAG (100 nM) and lestaurtinib (100 nM) in the presence of sublethal dose of cisplatin (A549^{cisR}: 2 µg/ml) for cell viability and increasing concentrations of cisplatin for IC₅₀ for 48 h. Cell viability and cisplatin IC₅₀ were assessed by trypan blue exclusion and CellTiter-Glo assay, respectively. Data are mean ± SD from three technical replicates and representative of three independent biological experiments (A) and from three biological replicates (B). Statistical analysis was performed by one-way ANOVA (***)*P*<0.005; ****)*P*<0.0001).



Supplemental Figure 10. Body weight, organ histology, and tumor Ki-67 staining of mice treated with vehicle control, lestaurtinib, 17-AAG, and combination. Nude mice were treated with cisplatin (5 mg/kg; intraperitoneal (i.p.) injection; twice a week), 17-AAG (50 mg/kg; i.p. injection; 5 times a week), and lestaurtinib (20 mg/kg; subcutaneous injection; 5 times a week) for 29 days. **(A)** Body weights were measured every 5-6 days during treatment. **(B)** Hematoxylin and eosin (H&E) stained tissue histology of representative mice are shown. Scale bars represent 50 μ m. **(C)** Effect of cisplatin treatment with the combination of 17-AAG and lestaurtinib on tumor proliferation of lung cancer PDX mice. Proliferation of the PDX tumors was assessed by Ki-67 IHC staining. Scale bars represent 50 μ m. n=5 mice/group. p values were determined by two-tailed Student's *t* test (ns: not significant). Data shown are representative of five biological replicates for (B) and (C).

	17-AAG [nM]		Lestaurinib [nM]		17-AAG [nM] + lestaurinib [nM]		
	Dose	Cytotoxicity effect	Dose	Cytotoxicity effect	Dose	Fraction affected (Fa)	Combination Index (CI)
KB-3-1 ^{cisR}	25	0.06412	25	0.09275	12.5 + 12.5	0.08448	1.00785
	50	0.10472	50	0.18320	25 + 25	0.14512	1.24977
	100	0.44943	100	0.50224	50 + 50	0.55370	0.53017
	200	0.59323	200	0.61555	*100 + 100	0.79001	0.44930
	300	0.65571	300	0.67830	150 + 150	0.81391	0.59999
	400	0.73818	400	0.72470	200 + 200	0.83597	0.71096
	Dm: 170.92, r=0.977		Dm: 149.59, r=0.979		Dm: 114.10, r=0.976		
A549 ^{cisR}	25	0.08017	25	0.06475	12.5 + 12.5	0.05225	1.79686
	50	0.30879	50	0.16201	25 + 25	0.11486	1.77409
	100	0.43312	100	0.56839	50 + 50	0.46330	0.74790
	200	0.58744	200	0.60056	*100 + 100	0.79268	0.44298
	300	0.66111	300	0.66574	150 + 150	0.81730	0.58462
	400	0.75193	400	0.71908	200 + 200	0.82872	0.73116
	Dm: 146.65, r=0.975		Dm: 155.25, r=0.955		Dm: 127.90, r=0.981		
A2780 ^{cisR}	50	0.09329	50	0.07989	25 + 25	0.05727	1.31982
	100	0.19537	100	0.19679	50 + 50	0.16861	1.16717
	200	0.38055	200	0.42671	100 + 100	0.44136	0.93085
	300	0.57814	300	0.59962	150 + 150	0.63762	0.81304
	400	0.64046	400	0.65788	*200 + 200	0.74698	0.76447
	500	0.72794	500	0.75133	250 + 250	0.78434	0.83014
	Dm: 258.92, r=0.997		Dm: 245.31, r=0.999		Dm: 230.75, r=0.999		
PCI-15A ^{cisR}	25	0.07326	50	0.07259	12.5 + 25	0.09881	0.79795
	50	0.17736	100	0.19370	25 + 50	0.18646	0.96851
	100	0.37086	200	0.33997	50 + 100	0.47526	0.76451
	150	0.56936	300	0.51134	*75 + 150	0.67642	0.65164
	200	0.65689	400	0.58817	100 + 200	0.69674	0.81515
	250	0.71874	500	0.69812	125 + 250	0.73638	0.89299
	Dm: 133.05, r=0.999		Dm: 294.81, r=0.997		Dm: 169.07, r=0.989		

Supplemental Table. 1. Synergistic combination of 17-AAG and lestaurinib. Dm: Median effect dose. Blue: Combination that resulted in synergism. *Combination providing the lowest CI value in each cell line.